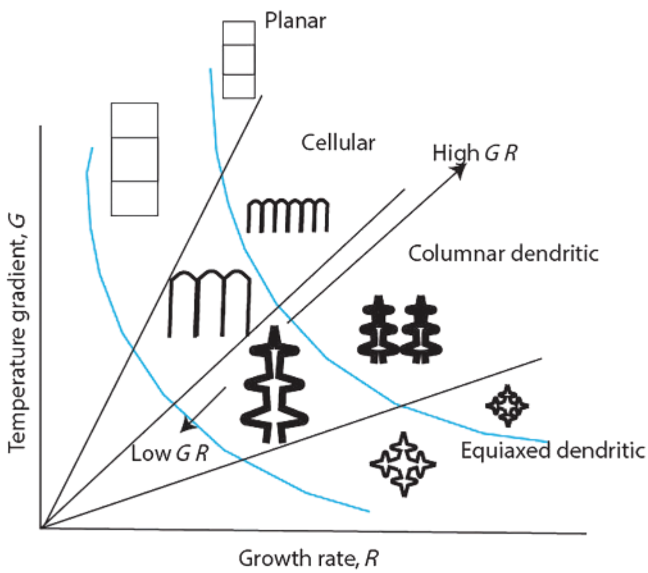

Figure 1.30 Schematic showing the effect of the temperature gradient (*G*) and the solidification speed (*R*) on the morphology and size of the grains in FZ.

in detail in the following chapters for arc welding processes, laser beam welding, resistance welding, and solid-state welding.

The mechanical properties of the weld depend on the microstructure. The microstructure of the FZ is cast, which consists of dendrites or columnar grains. Equiaxed grains may also appear in the weld zone, which is favored over the columnar or dendritic grains. It is shown that the equiaxed grains result in a higher ductility of the weld without any influence on the tensile strength [72]. The fine equiaxed structure provides more grain boundaries, which act as dislocation barriers, causing an increase in the yield strength (σ_y) according to the Hall–Petch equation [73].

$$\sigma_y = \sigma_0 + k.d^{-0.5} \tag{1.17}$$

where σ_0 is the opposite shear stress to the movement of dislocation inside the grain, k is a material constant representing the degree of difficulty to produce grain dislocation, and d is the grain diameter. The grain structure may also affect the mechanical properties through other mechanisms. For example, segregation of the alloying elements that cause hot cracking can also affect the failure mechanism of the joint in loading. Segregation is influenced by the grain structure, as discussed before. Along with the grain size and morphology, other mechanisms such as precipitation hardening, solution hardening, and strain hardening need to be considered in analyzing the mechanical properties of the joint.

In addition to thermal history, the nucleation particles affect the mechanical properties through modification of the solidification structure [74]. The metallographic images of the failed tensile specimens from the weld cross sections

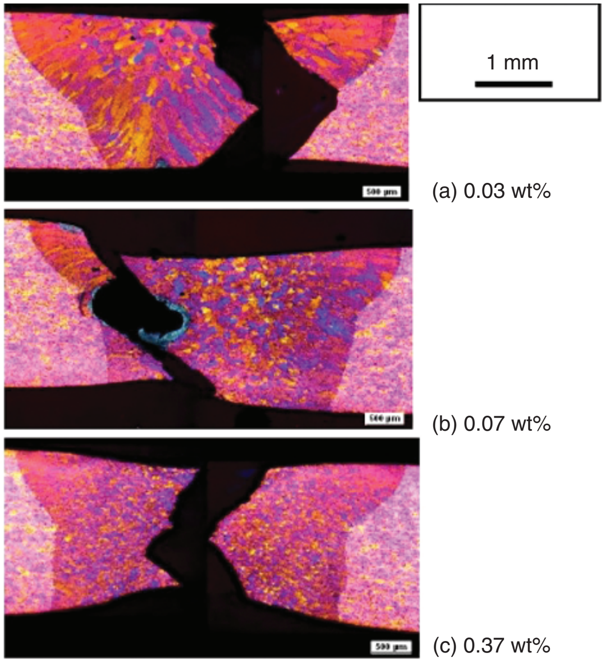

Figure 1.31 Metallographic images of the failed tensile specimens from the weld cross sections of three AA6082Al alloys with three different Ti content welded by laser welding [74]/DVS Media GmbH.

of three AA6082Al alloys with three different Ti content welded by laser welding are shown in Figure 1.31. At low Ti content, the FZ boundary consists of coarse columnar grains, where their boundary act as the fracture site during tensile testing. By 0.07% Ti addition, the fracture occurs along the boundary between the columnar and equiaxed grains. By 0.37% Ti, a full fine-equiaxed grain structure is developed, which promotes higher plastic deformation. The fracture occurs in the middle of the weld zone. The yield strength and ultimate tensile strength (UTS) of three specimens differ slightly, but the elongation of the weld to the fracture is highest in the specimen with the highest amount of Ti. The underlying mechanism by which the failure of the weld is influenced is the segregation and hot cracking caused by the grain structure. The degree of segregation is higher in coarse and columnar grains than the fine and equiaxed ones, as mentioned before. This explains the fracture locations observed in Figure 1.31. The mechanism of grain modification by adding nucleation particles is discussed in more detail in Chapter 2.

The thermal cycle not only influences the microstructure and mechanical properties, but also the distortion and residual stresses during welding. The distortion of Al alloys during welding is higher than steel due to its higher heat conductivity and higher thermal expansion coefficient. There are some basic laws that are practical for avoiding distortion during welding. For fillet welds, two simultaneous welding on both sides reduces the angular distortion. The seam welds, which cause the highest stiffness on the structure, should be performed last. The butt welds should be done before the filler welds [75].

1.4 Welding of Aluminum to Other Metals

A high demand exists for joining of Al to other metals such as steel, magnesium, and titanium, mainly for structural reasons. Welding of Al to copper is also gaining attention for electrical purposes, and hence, Al usage in the energy sector is increasing. The main challenge of welding Al to these materials is the formation of thick intermetallic compounds (IMCs), which are brittle and degrade the mechanical properties of the joint [76]. Usually, the interface is composed of one or more IMC layers at the interface. However, this layer is not always uniform, and its shape and morphology depend on the process and its parameters. The mechanical properties of the joint are highly influenced by the thickness and distribution of IMC as well as the direction of the applied load with respect to the interface [77, 78]. Dependency of the joint strength to the IMC thickness is depicted in Figure 1.32, which shows that while IMCs formation is necessary to establish a joint, its growth needs to be controlled to maintain its thickness in an optimum range.

The thickness of the IMC layer (d_{IMC}) is estimated by the following relationship

$$d_{IMC} = Dt^n \tag{1.18}$$

where D is the diffusion coefficient, t is time, and n is a constant whose value depends on the controlling factor of the growth, diffusion or reaction [79]. In dissimilar joints, the microstructures of the parent materials are not as decisive as the IMC layer, as this layer is the weakest point that controls the mechanical behavior. The mechanisms of IMC formation in fusion welding and solid-state welding processes are discussed in the following chapters.

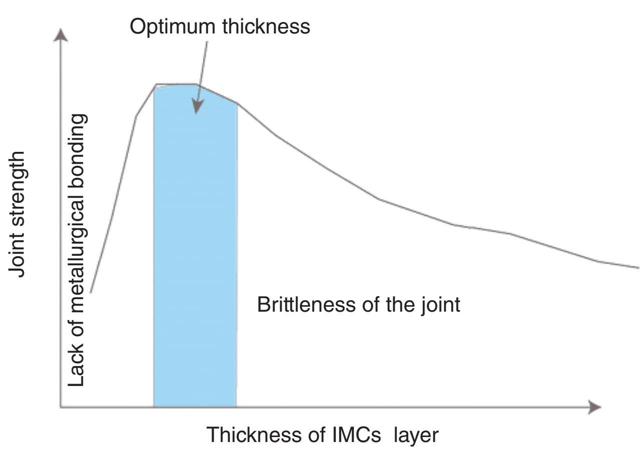

Figure 1.32 Dependency of the joint strength to the IMC thickness.

References

1 Murphy, A., McCune, W., Quinn, D. et al. (2007). The characterisation of friction stir welding process effects on stiffened panel buckling performance. *Thin-Walled Structures* 45 (3): 339–351.
2 Schulze, G. (2004). *Die Metallurgie des Schweißens: Eisenwerkstoffe—Nichteisenmetallische Werkstoffe*. Springer.
3 Dorn, L. (1998). Schweißverhalten von Aluminium und seinen Legierungen. *Materials Science and Engineering Technology* 29 (8): 412–423.
4 Zhang, P., Jia, Z., Yu, Z. et al. (2021). A review on the effect of laser pulse shaping on the microstructure and hot cracking behavior in the welding of alloys. *Optics Laser Technology* 140: 107094.
5 Srikanth, T., Surendran, S., Balaganesan, G. et al. (2017). Response of CMT welded aluminum AA5086-H111 to AA6061-T6 plate with AA4043 filler for ballistic. *Procedia Engineering* 194: 522–528.
6 Gould, J. (2012). Joining aluminum sheet in the automotive industry – a 30 year history. *Welding Journal* 91 (1): 23–34.
7 Sun, T., Franciosa, P., Sokolov, M. et al. (2020). Challenges and opportunities in laser welding of 6xxx high strength aluminium extrusions in automotive battery tray construction. *Procedia CIRP* 94: 565–570.
8 Abioye, T.E., Olanipekun, E., and Anasyida, A.S. (2022). Prediction of the hardness of pulverized glass waste-reinforced aluminium alloy 6061-T6 friction stir welded joint. *International Journal of Engineering Research in Africa* 62: 31–42.
9 Merino, J., Patzelt, A., Steinacher, A. et al. (2017). Ariane 6-Tanks and structures for the new european launcher. *Deutscher Luft- und Raumfahrtkongress*, München. Deutsche Gesellschaft für Luft-und Raumfahrt-Lilienthal-Oberth eV.
10 Cai, C., Shuang, H., Chen, H. et al. (2019). The influences of Ar—He shielding gas mixture on welding characteristics of fiber laser-MIG hybrid welding of aluminum alloy. *Optics & Laser Technology* 113: 37–45.
11 Lee, H.-K., Park, S.-h., and Kang, C.-Y. (2015). Effect of plasma current on surface defects of plasma-MIG welding in cryogenic aluminum alloys. *Journal of Materials Processing Technology* 223: 203–215.
12 Kashaev, N., Ventzke, V., and Çam, G. (2018). Prospects of laser beam welding and friction stir welding processes for aluminum airframe structural applications. *Journal of Manufacturing Processes* 36: 571–600.
13 Hobbacher, A. (2016). *Recommendations for Fatigue Design of Welded Joints and Components*, vol. 47. Springer.
14 Hossain, I., Bhowmik, A., Pattanaik, A. et al. (2024). Computational investigation of plasma arc welding process for aluminium alloys. *Engineering Research Express* 6 (2): 025541.
15 Dobosy, Á., Gáspár, M., and Török, I. (2018). Resistance spot welding of 7075 aluminium alloy. *Proceedings of the Second Vehicle and Automotive Engineering 2: VAE2018*, Miskolc, Hungary. Springer.
16 Dilthey, U. (2006). *Schweißtechnische Fertigungsverfahren 2: Verhalten der Werkstoffe beim Schweißen*. Springer-Verlag.

17 Kovács, J. and Lukács, J. (2022). Investigation of the Possibility for Compensating the HAZ Softening of AA7075-T6. *Periodica Polytechnica Mechanical Engineering* 66 (3): 207–212.

18 Liu, T., Mu, Z., Hu, R. et al. (2019). Sinusoidal oscillating laser welding of 7075 aluminum alloy: hydrodynamics, porosity formation and optimization. *International Journal of Heat and Mass Transfer* 140: 346–358.

19 Enz, J. (2012). *Laserstrahlschweissen von hochfesten Aluminium-Lithium-Legierungen*. Springer.

20 Warner, T. Recently-developed aluminium solutions for aerospace applications. In Materials Science Forum. 2006. *Trans Tech Publications.*

21 Zhang, J., Feng, X.S., Gao, J.S. et al. (2018). Effects of welding parameters and post-heat treatment on mechanical properties of friction stir welded AA2195-T8 Al–Li alloy. *Journal of Materials Science & Technology* 34 (1): 219–227.

22 Avilov, V., Gumenyuk, A., Lammers, M. et al. (2012). PA position full penetration high power laser beam welding of up to 30 mm thick AlMg3 plates using electromagnetic weld pool support. *Science Technology of Welding Joining* 17 (2): 128–133.

23 Tang, G., Chen, H., Yang, X. et al. (2018). Effects of different welding process on the electronic temperature of plasma and weld shape during laser-MIG hybrid welding of A7N01P-T4 aluminum alloy. *Journal of Laser Applications* 30 (2): 022002.

24 Balanovskii, A.E. (2019). A new mechanism of interaction between a welding arc discharge of reverse-polarity direct current and an aluminum surface. *High Temperature* 57: 784–797.

25 Pellone, L., Inmake, G., Hong, K.-M. et al. (2019). Effects of interface gap and shielding gas on the quality of alloy AA6061 fiber laser lap weldings. *Journal of Materials Processing Technology* 268: 201–212.

26 Feng, J., Zhang, P., Yan, H. et al. (2023). Application of laser welding in electric vehicle battery manufacturing: a review. *Coatings* 13 (8): 1313.

27 Kang, Y., Zhan, X.H., and Liu, T. (2019). Effect of welding parameters on porosity distribution of dual laser beam bilateral synchronous welding in 2219 aluminum alloy T-joint. *Journal of Adhesion Science and Technology* 33 (23): 2595–2614.

28 Chen, Q., Ge, H., Yang, C. et al. (2017). Study on pores in ultrasonic-assisted TIG weld of aluminum alloy. *Metals* 7 (2): 53.

29 Ardika, R.D., Triyono, T., and Muhayat, N. (2021). A review porosity in aluminum welding. *Procedia Structural Integrity* 33: 171–180.

30 He, E., Liu, J., Lee, J. et al. (2018). Effect of porosities on tensile properties of laser-welded Al–Li alloy: an experimental and modelling study. *The International Journal of Advanced Manufacturing Technology* 95: 659–671.

31 Yan, S., Zhu, Z., Ma, C. et al. (2019). Porosity formation and its effect on the properties of hybrid laser welded Al alloy joints. *The International Journal of Advanced Manufacturing Technology* 104: 2645–2656.

32 Vyskoč, M., Sahul, M., and Sahul, M. (2018). Effect of shielding gas on the properties of AW 5083 aluminum alloy laser weld joints. *Journal of Materials Engineering and Performance* 27: 2993–3006.

33 Han, X., Yang, Z., Ma, Y. et al. (2020). Porosity distribution and mechanical response of laser-MIG hybrid butt welded 6082-T6 aluminum alloy joint. *Optics & Laser Technology* 132: 106511.

34 Chen, L., Wang, C., Xiong, L. et al. (2020). Microstructural, porosity and mechanical properties of lap joint laser welding for 5182 and 6061 dissimilar aluminum alloys under different place configurations. *Materials & Design* 191: 108625.

35 Miyagi, M., Kawahito, Y., Wang, H. et al. (2018). X-ray phase contrast observation of solidification and hot crack propagation in laser spot welding of aluminum alloy. *Optics Express* 26 (18): 22626–22636.

36 Rappaz, M., Drezet, J.-M., and Gremaud, M. (1999). A new hot-tearing criterion. *Metallurgical and Materials Transactions A* 30: 449–455.

37 Tang, Z. and Vollertsen, F. (2014). Influence of grain refinement on hot cracking in laser welding of aluminum. *Welding in the World, Le Soudage Dans Le Monde* 58: 355–366.

38 Wang, X.J., Lu, F., Wang, H.-P. et al. (2015). Experimental and numerical analysis of solidification cracking behaviour in fibre laser welding of 6013 aluminium alloy. *Science and Technology of Welding & Joining* 20 (1): 58–67.

39 Pumphrey, W.I. and Moore, D.C. (1948). A consideration of the nature of brittleness at temperatures above the solidus in castings and welds in aluminium alloys. *Journal of the Institute of Metals* 75: 235–256.

40 Bielenin, M. (2021). *Prozessstrategien zur Vermeidung von Heißrissen beim Schweißen von Aluminium mit pulsmodulierbaren Laserstrahlquellen*. BoD–Books on Demand.

41 Kubo, K. and Pehlke, R.D. (1985). Mathematical modeling of porosity formation in solidification. *Metallurgical and Materials Transactions B* 16: 359–366.

42 Kou, S. (2003). *Welding Metallurgy*, 223–225. John Wiley & Sons.

43 Kou, S., Firouzdor, V., and Haygood, I.W. (2011). Hot cracking in welds of aluminum and magnesium alloys. *Materials Science Engineering* 3–23.

44 Jennings, P.H. (1949). *Hot-shortness of Some High-purity Alloys in the Systems Aluminium–Copper–Silicon and Aluminium–Magnesium–Silicon*. Aluminium Development Association.

45 Coniglio, N. and Cross, C.E. (2009). Mechanisms for solidification crack initiation and growth in aluminum welding. *Metallurgical and Materials Transactions A* 40: 2718–2728.

46 Tian, Y., Robson, J.D., Riekehr, S. et al. (2016). Process optimization of dual-laser beam welding of advanced Al–Li alloys through hot cracking susceptibility modeling. *Metallurgical Materials Transactions A* 47: 3533–3544.

47 Hagenlocher, C., Weller, D., Weber, R. et al. (2019). Analytical description of the influence of the welding parameters on the hot cracking susceptibility of laser beam welds in aluminum alloys. *Metallurgical and Materials Transactions A* 50: 5174–5180.

48 Von Witzendorff, P., Kaierle, S., Suttmann, O. et al. (2015). In situ observation of solidification conditions in pulsed laser welding of AL6082 aluminum alloys to evaluate their impact on hot cracking susceptibility. *Metallurgical and Materials Transactions A* 46: 1678–1688.

49 Hagenlocher, C., Stritt, P., Weber, R. et al. (2018). Strain signatures associated to the formation of hot cracks during laser beam welding of aluminum alloys. *Optics and Lasers in Engineering* 100: 131–140.

50 Coniglio, N., Cross, C.E., Michael, T. et al. (2008). Defining a critical weld dilution to avoid solidification cracking in aluminum. *Welding Journal* 87 (8): 237s–247s.

51 Wei, H., Chen, J.S., Wang, H.-P. et al. (2016). Thermomechanical numerical analysis of hot cracking during laser welding of 6XXX aluminum alloys. *Journal of Laser Applications* 28 (2): 022405.

52 Norouzian, M., Elahi, M.A., and Plapper, P. (2023). A review: suppression of the solidification cracks in the laser welding process by controlling the grain structure and chemical compositions. *Journal of Advanced Joining Processes* 7 (9): 100139.

53 Hagenlocher, C., Weller, D., Weber, R. et al. (2019). Reduction of the hot cracking susceptibility of laser beam welds in AlMgSi alloys by increasing the number of grain boundaries. *Science and Technology of Welding & Joining* 24 (4): 313–319.

54 Easton, M.A., Grandfield, J., John, S., D. et al. (2006). The effect of grain refinement and cooling rate on the hot tearing of wrought aluminium alloys. *Materials Science Forum* 519–521: 1675–1680. Trans Tech Publications.

55 Soysal, T. (2021). A criterion to find crack-resistant aluminium alloys to avoid solidification cracking. *Science and Technology of Welding & Joining* 26 (2): 99–105.

56 Liu, J. and Kou, S. (2016). Crack susceptibility of binary aluminum alloys during solidification. *Acta Materialia* 110: 84–94.

57 Liu, J. and Kou, S. (2017). Susceptibility of ternary aluminum alloys to cracking during solidification. *Acta Materialia* 125: 513–523.

58 Liu, J. and Kou, S. (2015). Effect of diffusion on susceptibility to cracking during solidification. *Acta Materialia* 100: 359–368.

59 Malekshahi Beiranvand, Z., Ghaini, F.M., Naffakh-Moosavy, H. et al. (2019). An analytical model for prediction of solidification cracking susceptibility in aluminum alloys taking into account the effect of solidification rate. *Metallurgical Transactions A* 50: 2835–2846.

60 Holzer, M., Hofmann, K., Mann, V. et al. (2016). Change of hot cracking susceptibility in welding of high strength aluminum alloy AA 7075. *Physics Procedia* 83: 463–471.

61 Deng, A., Chen, H., Zhang, Y. et al. (2023). Prediction of the influence of welding metal composition on solidification cracking of laser welded aluminum alloy. *Materials Today Communications* 35: 105556.

62 Wan, Z., Meng, D., Zhao, Y. et al. (2022). Improvement in tensile properties of 2219-T8 aluminum alloy TIG welding joint by PMZ local properties and stress distribution. *Journal of Manufacturing Processes* 839: 142863.

63 Jula, M., Dehmolaei, R., and Ranjbar, K. (2023). Softening, hardening, and precipitation evolution of the AA6082-T651 heat-affected zone caused by thermal cycles during and after welding. *Metals and Materials International* 29 (12): 3664–3678.

64 Pérez, J.S., Ambriz, R.R., Curiel López, F.F. et al. (2016). Recovery of mechanical properties of a 6061-T6 aluminum weld by heat treatment after welding. *Metallurgical and Materials Transactions A* 47: 3412–3422.

65 Cheng, J., Song, G., Zhang, X. et al. (2021). Review of techniques for improvement of softening behavior of age-hardening aluminum alloy welded joints. *Materials (Basel)* 14 (19): 5804.

66 Jie, Y., Wang, G., Li, S.-k. et al. (2019). Effect of post-weld heat treatment on microstructure and mechanical properties of welded joints of 6061-T6 aluminum alloy. *Transactions of Nonferrous Metals Society of China* 29 (10): 2035–2046.

67 Zhang, Y., Li, H., Li, Z. et al. (2021). Quantitative analysis of the solute redistribution and precipitate of Al–Mg–Si series alloys resistance spot welds after post–weld heat treatment. *Journal of Materials Research and Technology* 15: 5906–5919.

68 Chen, Y., Liu, H., and Feng, J. (2006). Friction stir welding characteristics of different heat-treated-state 2219 aluminum alloy plates. *Materials Science and Engineering: A* 420 (1–2): 21–25.

69 Aydın, H., Bayram, A., and Durgun, I. (2010). The effect of post-weld heat treatment on the mechanical properties of 2024-T4 friction stir-welded joints. *Materials & Design* 31 (5): 2568–2577.

70 Elangovan, K. and Balasubramanian, V. (2008). Influences of post-weld heat treatment on tensile properties of friction stir-welded AA6061 aluminum alloy joints. *Materials Characterization* 59 (9): 1168–1177.

71 Geng, S., Jiang, P., Shao, X. et al. (2020). Heat transfer and fluid flow and their effects on the solidification microstructure in full-penetration laser welding of aluminum sheet. *Journal of Materials Science & Technology* 46: 50–63.

72 Wang, L., Gao, M., Zhang, C. et al. (2016). Effect of beam oscillating pattern on weld characterization of laser welding of AA6061-T6 aluminum alloy. *Materials & Design* 108: 707–717.

73 Saifudin, S., Muhayat, N., Surojo, E. et al. (2022). Mitigation of porosity and residual stress on car body aluminum alloy vibration welding: a systematic literature review. *Automotive Experiences* 5 (3): 477–493.

74 Tang, Z., Schempp, P., Seefeld, T. et al. (2011). *Kornfeinung beim WIG-und Laserstrahlschweißen von Aluminiumlegierungen*. DVS-Verlag.

75 Nölle, P. (2011). Verzugarmes Schweißen von Aluminiumwerkstoffen. *Lightweight Design* 4 (2): 58–63.

76 Beygi, R., Kazeminezhad, M., and Kokabi, A.H. (2014). Microstructural evolution and fracture behavior of friction-stir-welded Al—Cu laminated composites. *Metallurgical and Materials Transactions A* 45: 361–370.

77 Beygi, R., Talkhabi, A.A., Mehrizi, M.Z. et al. (2023). A novel lap-butt joint design for FSW of aluminum to steel in Tee-configuration: joining mechanism, intermetallic formation, and fracture behavior. *Metals* 13 (6): 1027.

78 Beygi, R., Carbas, R.J.C., Marques, E.A.S. et al. (2023). Mechanism of toughness enhancement of brittle fracture by intermittent η-intermetallic in Al/Cu joint made by FSW. *Materials Science and Engineering A* 145907.

79 Springer, H., Kostka, A., Payton, E. et al. (2011). On the formation and growth of intermetallic phases during interdiffusion between low-carbon steel and aluminum alloys. *Acta Materialia* 59 (4): 1586–1600.